Desantes Fernández, JM.; López, JJ.; Redón Lurbe, P.; Arregle, JJP. (2012). Evaluation of the Thermal NO formation mechanism under low-temperature diesel combustion conditions. International Journal of Engine Research. 13(6):531-539. doi:10.1177/1468087411429638.

Evaluation of the Thermal NO formation mechanism under low-temperature diesel combustion conditions

José María Desantes[1], José Javier López[1], Pau Redón[1] and Jean Arrégle[2]

Abstract

Over the past two decades, the amount of exhaust gas pollutants emissions has been significantly reduced due to the severe emission legislation imposed in most countries worldwide. Initial strategies simply required the employment of simple after-treatment and engine control devices; however, as the restrictions become more stringent, these strategies are evolving in the development of different combustion modes, specially characterized by having low-temperature combustion characteristics. These new working conditions demand the need to check the suitability of the current NO predictive models that coexist nowadays under standard diesel combustion characteristics, paying closer attention to the Thermal mechanism. In order to do so, a common chemical-kinetic software was employed to simulate, for n-heptane and methane fuels, fixed local conditions (standard diesel and low-temperature combustion) described by constant pressure, relative mixture fraction, oxygen mass fraction and initial and final reaction temperature. The study reflects a common trend between all the studied cases, independently of the considered local conditions, making it applicable to more complex situations such as real NO formation processes in diesel sprays. This relationship was characterized by a fourth-degree polynomial equation capable of substantially improving the NO prediction by just using the Thermal NO predictive model.

Keywords

Low-temperature combustion, NO formation mechanism, chemical-kinetic modelling, diesel spray, diesel engines

Introduction

Over the past two decades, the amount of exhaust gas pollutants emissions has been significantly decreased due to the severe emission legislation imposed in Europe with the well-known Euro Emission Standards, as can be seen from Table 1. A similar situation can be found in other countries worldwide.

Initially, the accomplishment of the standards was fulfilled by using simple after-treatment and engine control devices coupled with standard diesel combustion (STD) characteristics. Nowadays, the current (Euro 5) and future (Euro 6) restrictions imply the need to change the diesel combustion process itself. In order to do so, many research and development efforts have been focused on reinventing the way diesel fuel is burnt inside an internal combustion engine. Analysing an equivalence ratio–temperature map,[1] where the soot and NO formation regions are delimited, it is appreciable that the new research field has to focus on the left side of the diagram represented in Figure 1. This area corresponds to low local temperature characteristics, and much research is now taking place developing new combustion modes, like homogeneous charge compression ignition (HCCI), premixed charge compression ignition (PCCI) and proper low-temperature combustion (LTC).

Until now, diesel engines have worked under STD conditions, mainly characterized by high local temperatures and equivalence ratios. Due to the extended use of this type of combustion, a conceptual model had to be developed to help explain the different factors affecting

[1]CMT-Motores Térmicos, Universitat Politècnica de València, Spain
[2]Departamento de Máquinas y Motores Térmicos, Universitat Politècnica de València, Spain

Corresponding author:
P Redón, CMT-Motores Térmicos, Universidad Politécnica de Valencia, Camino de Vera s/n. 46022, Valencia, Spain.
Email: paredlur@mot.upv.es

Table 1. Euro emission standards for diesel passenger cars.

Diesel passenger cars					
Emission standard	Date	CO (g/km)	NOx (g/km)	HC + NOx (g/km)	PM (g/km)
Euro 1	July 1992	2.72	–	0.97	0.14
Euro 2	January 1996	1	–	0.7	0.08
Euro 3	January 2000	0.64	0.5	0.56	0.05
Euro 4	January 2005	0.5	0.25	0.3	0.025
Euro 5	September 2009	0.5	0.18	0.26	0.005
Euro 6	September 2014	0.5	0.08	0.17	0.005

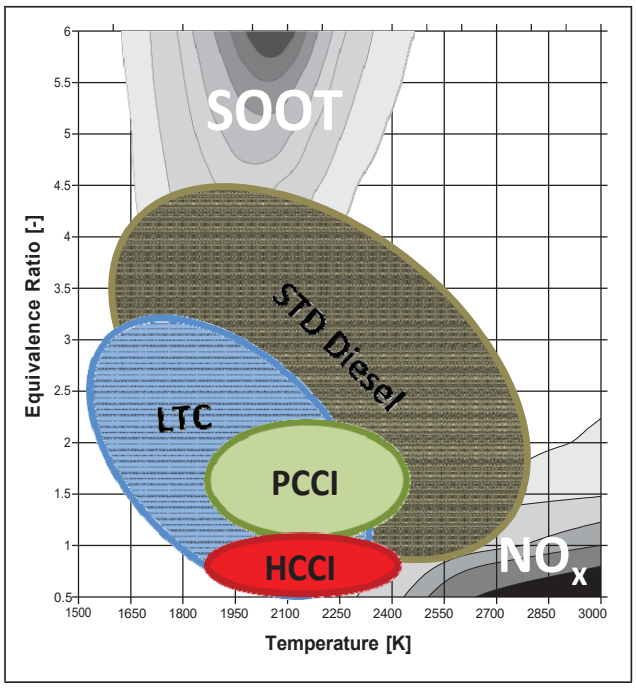

Figure 1. Predominant f–T working conditions for several new combustion modes based on Dronniou et al.[1]

the process. For the past two or three decades, several authors worked on the topic, trying to build up a model but, due to its complexity, it was not until optical measuring tools were improved that it was possible to configure a suitable conceptual model. The most widely

Figure 2.

In contrast, the new combustion modes, characterized by LTC diesel conditions, remain mainly unknown due to the youth of these modes and the complex chemical and physical processes involved. However, a recent study performed by Musculus[3] has started to reveal some interesting guidelines concerning diesel spray structure under these conditions and have been summarized as 'an extension of Dec's model'.

Due to the degree of uncertainty still remaining in this field, a possible method for dealing with this lack of knowledge is to extrapolate the well-known principles of STD to LTC. In the present study, a simplified version of Dec's model is going to be used as a

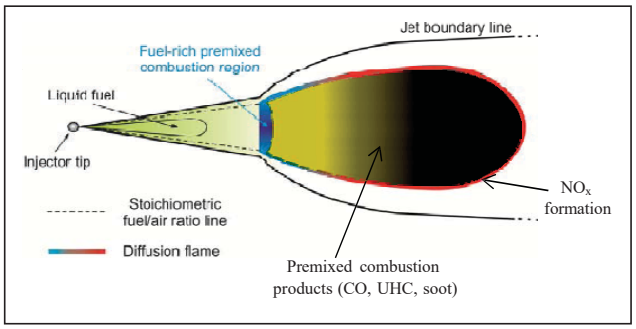

Figure 2. Stabilized diffusive flame scheme based on Dec's diffusive flame conceptual model.[2]

reference, illustrated in Figure 3, in order to review the different processes involved in the NO formation phenomenon, at STD conditions.

Using this model as a scientific guideline will help understand the processes, simplifications and evolution of the fuel mass fraction (Y_f) (defined as a function of mixture fraction (Z)), oxygen mass fraction (Y_{O2}), temperature (T) and NO formation rate as the flame progresses.

The process starts when liquid fuel, injected into the combustion chamber at a temperature of approximately 350 K, starts to undergo atomization (break up

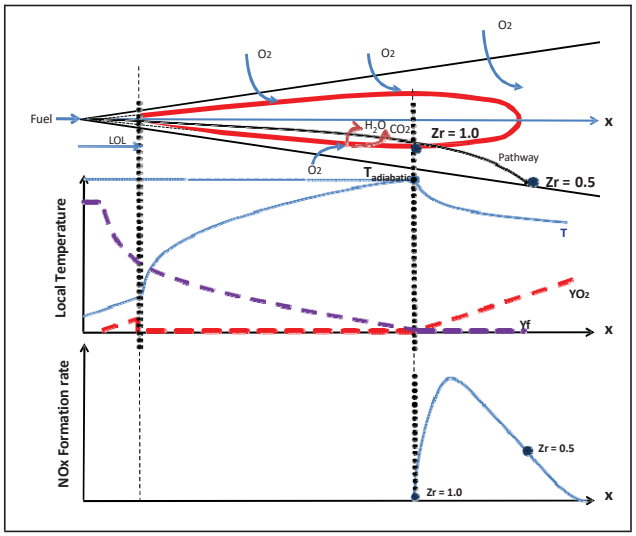

Figure 3. Fuel package position evolution.

of droplets into smaller ones) and a mixing phenomenon with entrained hot air, located inside the combustion chamber, due to the momentum flux with which it has been injected. Both processes cause an increase in the fuel's temperature, enhancing the fuel's evaporation, until it reaches the evaporative liquid length (L_{liq}). From this distance on, the vapour continues to mix with air, from the surroundings, until it reaches autoignition conditions, causing a fuel-rich premixed combustion reaction at a distance from the nozzle known as the lift-off length (LOL). This reaction causes the formation of small hydrocarbon chains (C_2H_2, C_2H_4, C_3H_3), partially burned products (CO), a temperature increase and consumption of all the oxygen entrained previously.

Next, the different products enter the internal zone of the diffusive flame where it continues to mix with burned gases coming from the flame front. At this point, no oxygen is present due to the diffusive flame front, located around the flame's perimeter, which prevents it from entering. The lack of oxygen implies the lack of energy release in this region, even though the temperature continues to rise due to the mixing process with hot combustion products.

When these products reach the flame front, the remaining hydrocarbons and unburned products are completely burned, with the presence of oxygen, under stoichiometric conditions. This causes the release of the remaining energy still stored in the hydrocarbons and unburned products, increasing the temperature to 2700–3000 K in classical combustion conditions. It is beyond this region where the NO formation mechanisms are activated due to the presence of high temperatures and high oxygen content. However, the NO formation process under LTC conditions is likely to be formed throughout the jet cross-section, in the same relatively hot, oxygen available environments, where OH exists. Even though the NO formation scenario changes from LTC to STD conditions, it is worth mentioning that the results obtained from the present study show its independence of a particular scenario, LTC or STD.

Therefore, to study the formation of this pollutant, from a physical point of view, we must focus on all those variables and processes involved in diffusive flame combustion, such as oxygen content (Y_{O2}) and the influence of local temperatures.

In addition to understanding the physical principles, the chemical processes are gaining importance. Several authors have tried to study the chemical-kinetic aspects of the NO formation process. These investigations have concluded with several well-known chemical models classified into two main groups: those based on kinetic schemes and those based on chemical equilibrium hypotheses. Most of the models used nowadays are based on the latter principle and are mainly applicable for STD conditions. The most important ones are briefly described in the following paragraphs.

The Thermal mechanism was first postulated by Zeldovich in 1946[4] and nowadays is the most extended one in commercial computational fluid dynamics (CFD) softwares for emission studies. It has a strong temperature dependence and describes the formation of nitric oxides from the oxidation of atmospheric nitrogen, at relatively high temperatures, in fuel-lean environments.[5] An additional elementary reaction is often added in what is called the extended or modified Zeldovich mechanism. This last mechanism takes into account the NO formation due to oxygen and hydrogen radicals.

The Prompt mechanism was reported by Fenimore[6] and considers the NO formation by the reaction of atmospheric nitrogen with hydrocarbon radicals in fuel-rich regions to form cyano compounds and amines. These are then converted to intermediate compounds that ultimately form NO. The reaction where hydrocarbon radicals react with atmospheric nitrogen is the rate limiting and the primary path, as it is believed that 90% of NO Prompt formed is via HCN.

The N_2O intermediate mechanism[7,8] considers the NO formation due to high pressures and lean fuel conditions and with a third-body reactant. The mechanism starts by the formation of N_2O from atmospheric nitrogen.

The fuel contribution mechanism[5,7,8] considers that NO is formed by the nitrogen bound in the fuel. Usually, it is assumed to proceed through the formation of HCN and/or NH_3, which are oxidized to NO while being competitively reduced to N_2.

Even if all these mechanisms have relevance in predicting the amount of NO formed under certain conditions, the predominant one for STD characteristics is the Thermal mechanism.[9–14] This mechanism offers scientists and engineers the opportunity to accurately predict up to 90% of the amount of NO formed with low computational cost.

On the other hand, when working at LTC conditions, the Thermal mechanism loses accuracy,[10–13,15] and others, such as Prompt and/or N_2O intermediate mechanisms, start to gain relevance. Therefore, new predictive tools, which take into account the widest possible range of operational conditions, are strongly required.

Objectives and methodology

The aim of this paper is to study the behaviour of NO formation mechanisms, particularly focusing on the Thermal mechanism, under STD and LTC local conditions. In order to do so, a parametric study was designed and executed using Chemkin Pro version.[16] Generally speaking, this consisted of varying the final reaction temperature (T_{end}) by modifying the amount of oxygen mass fraction (Y_{O2}) in the fuel–air mixture for a given fixed local condition, which is described by relative mixture fraction (Z_r) (mixture fraction and relative mixture fraction are explained in great detail by Peters[17]), constant pressure (P) and initial reaction

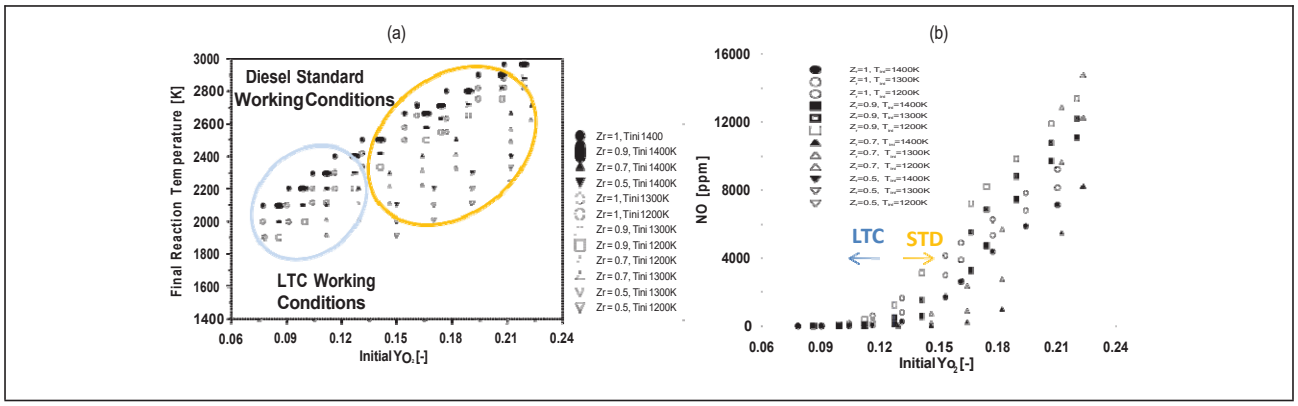

Figure 4. (a) End temperature of the considered working conditions, characterized by Zr and Tini. Calculations were performed using the equilibrium module of the Chemkin Pro package, considering constant pressure and enthalpy conditions. (b) Amount of NO formed for 1 ms for the considered working conditions characterized by Zr and Tini. Calculations were performed using the perfectly stirred reactor module of the Chemkin Pro package.

temperature (T_{ini}). This is shown in Figure 4(a) and (b), where all the fixed local conditions considered are plotted, with the STD and LTC regions.

The plot in Figure 4(a) was obtained using the equilibrium module of the Chemkin Pro package, considering constant pressure and constant enthalpy conditions. The equilibrium hypothesis will remove the time effect on the combustion process and reflects the expected flame temperature for a particular working condition. Additionally, the circles delimiting the STD and LTC regions were depicted using the same criterion (Y_{O2} 4 12.7%) to the one used in several research studies.[18–20]

In addition to the previous plot, the amount of NO formed, for 1 ms, was also plotted as a function of Y_{O2} using a perfectly stirred reactor (PSR) module (Figure 4(b)). In this case, no equilibrium hypothesis was employed due to the fact that the NO formation process is much slower compared to the temperature evolution and consequently substantial differences can appear between NO_{eq} and NO_{1ms}, especially under LTC conditions. This figure also relates the predicted amount of NO with the two studied combustion modes, LTC and STD, and with flame temperature values when coupled with Figure 4(a). As expected, lower initial oxygen concentrations cause a reduction in flame temperature and therefore lower formation of NO.

Detailed definitions of each of these variables are presented in Table 2. Special attention must be paid to the variable T_{ini}, which corresponds to the temperature given by the mixture of the injected fuel and the entrained hot air, if extrapolated to Dec's conceptual model. This means that the fuel-rich premixed combustion process is neglected due to the lack of NO formation at this stage.

Additional variables required to run the current analysis are a fuel surrogate, a chemical-kinetic model (skeletal, reduced or extended) and a reactor model, which describes the physics of the process.

Initially, the fuel surrogate chosen was n-heptane due to its similar cetane number with typical European diesel fuel and its popularity in simplified LTC diesel studies.[21] Then, in order to study the effects of a different fuel on the NO formation process, a second fuel surrogate was used, methane. Even though the use of these single-component fuel surrogates discards the process of NO formation by fuel contribution, due to the lack of nitrogen and aromatics content, these are

Table 2. Detailed definition of the variables used for the present study.

Variable	Definition	Variable range
Relative mixture fraction (Zr)	$Z_r = Z / Z_{st}$ $Z = (\text{mass } C_{local} - \text{mass } C_{oxid}) / (\text{mass } C_{fuel} - \text{mass } C_{oxid})$	0.5, 0.7, 0.9, 1
Oxygen mass fraction (Y_{o2})	$Y_{O2} = m_{O2} = (m_{oxid} + m_f)$ $m_{oxid} = m_{air} + m_{EGR}$ $Y_{O2\,atm} = 0.2313$	0.08–0.22
Fuel mass fraction (Y_f)	$Y_f = (Z - Z_{st}) / (1 - Z_{st})$	–
Initial reaction temperature (T_{ini})	Temperature reached when the hot entrained air mixes with the injected fuel	1200 K, 1300 K, 1400 K
Final reaction temperature (T_{end})	Temperature reached at the end of the reaction	2100–2970 K

widely used in simplified simulations. Nevertheless, future studies will analyse their effects on the NO formation process.

Regarding the chemical-kinetic mechanism, the December 2005 version of the San Diego model[22] was employed. This model was developed at the Mechanical Aerospace Engineering Department of the University of California in San Diego and incorporates n-heptane and methane oxidation chemistry, as well as NO formation chemistry (Thermal, Prompt and N_2O mechanisms) and other complementary sub-mechanisms, in total 58 chemical species and 264 chemical reactions.

In order to analyse the behaviour of the different mechanisms, several versions of this model were created, by the authors, and simulated one by one. Each version contained one of the three NO formation mechanisms, presented previously, and were named after the mechanism included in it (Thermal, Prompt, N_2O pathway and All). The All version of the San Diego model, which included all three mechanisms, was used as a reference (Total NO).

When characterizing the physical phenomenon behind the NO formation mechanisms, inside a diffusive flame, two possible scenarios can be considered. The first one implies the use of continuously varying conditions, such as in real diesel sprays processes, yielding realistic results, but with a high computational cost. The second scenario consists of considering fixed local conditions and consequently substantially simplifying the simulations. In the present study, the second scenario was considered, and a PSR was employed.

Finally, it is worth highlighting that, even though all of the simplifications assumed may seem to trivialize the present study, making it irrelevant for any practical application, as this study is developed, it will reflect interesting conclusions independently of this methodology.

Results and discussion

Individual results

Initially, three random cases were selected (Table 3) to study the contribution degree of the different mechanisms involved in the study. In order to do so, individual simulations of the different San Diego versions, Thermal, Prompt, N_2O and All, were performed for a characteristic combustion time of 1.0 ms. This combustion time was chosen based on two complementary criteria.

Table 3. Summary of the three random cases chosen from the parametric study performed.

Cases	Z_r	T_{end} (K)	Y_{O2} (-)	Y_f (-)	$NO_{version\ All,\tau=1\ ms}$ (ppm)
Case A	1	2200	0.09	0.026	66.9
Case B	1	2400	0.116	0.033	756.7
Case C	0.7	2200	0.129	0.025	254.8

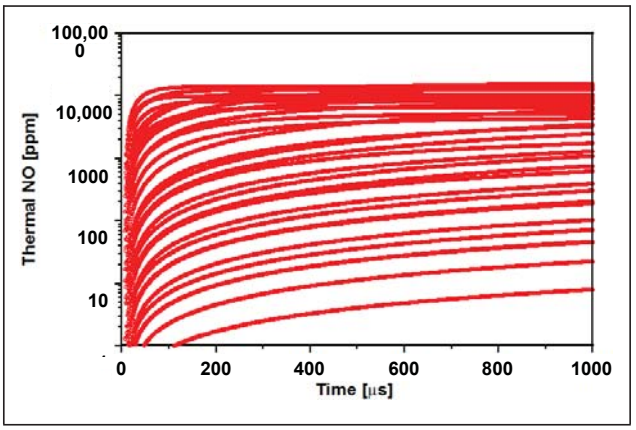

Figure 5. Time evolution of the Thermal NO formation mechanism for all the local conditions tested in the present study.

1. Equilibrium conditions, or close to them, for the majority of the local conditions studied. This fact is corroborated in Figure 5, where the whole NO formation processes of all the studied conditions are plotted. As expected, the quickest cases to reach the equilibrium state belong to STD conditions, where high NO formation is expected, and the slowest pertain to LTC. Despite the differences in speed, it is observed from this plot that by using this criterion, the great majority of the tested local conditions are in the equilibrium state or close to it.
2. Realistic combustion process time scales. These were of the order of the magnitude of the residence time of a fuel parcel in the NO formation region of a diffusion flame.

The next step was to plot the results obtained. The first plot in Figure 6 illustrates the differences between the predictive capabilities of each of the NO formation mechanisms studied for Case A. As can be observed, the Thermal mechanism still remains predominant, but with a lower predictive capability than for STD conditions. Additionally, it is worth highlighting the fact that the amount of NO formed by the three studied mechanisms do not sum up to the NO formed by the All version (Total NO). This can be explained due to the fact that all the mechanisms have to converge to a given NO value that is independent of chemical kinetics, the NO in the equilibrium state. Mathematically, it can be demonstrated that due to this fact, the sum of the three NO formation mechanism predictions do not add up to the All version prediction at any particular time.

Then, cases B and C (with different Z_r and T_{end}) were plotted focusing on the differences between the Thermal NO and the Total NO predictions. These are shown in Figure 6(b) using solid and dashed lines, respectively. From this plot, several interesting ideas

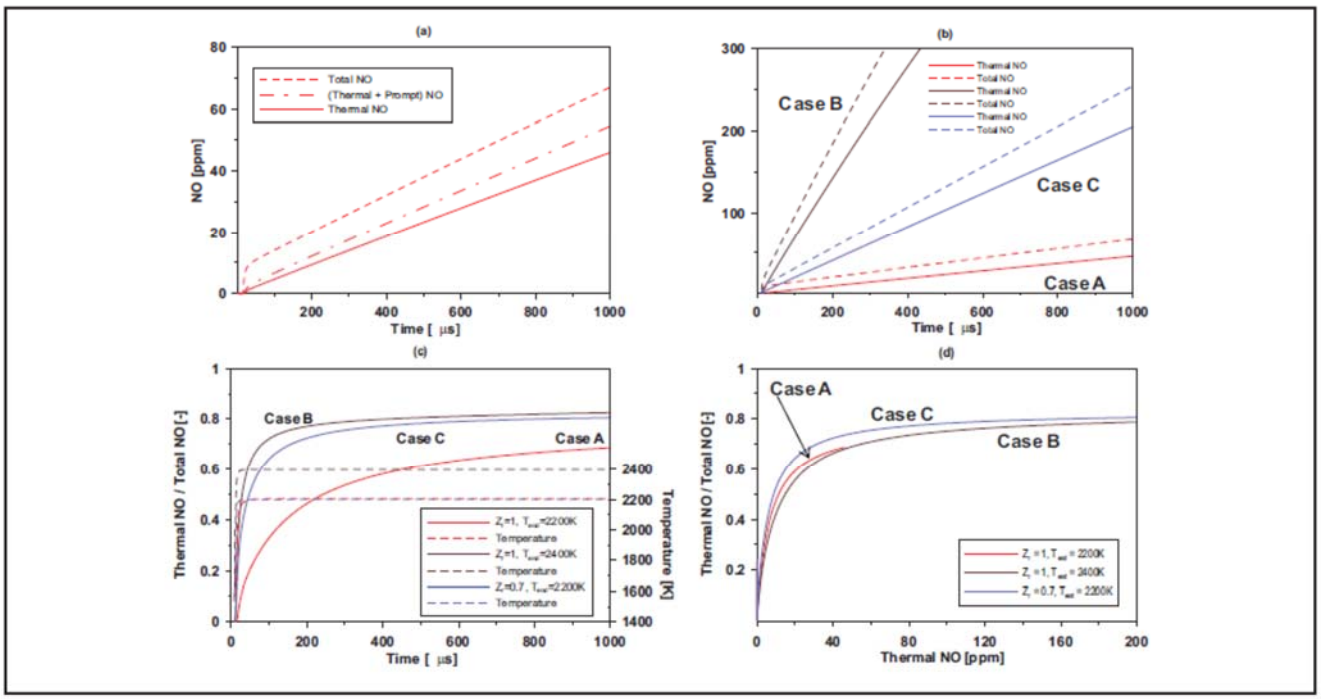

Figure 6. (a) Prediction of NO formation, for a particular local condition, depending on the different mechanisms considered. (b) Effect of the Z_r and T_{end} on the amount of NO formed, considering Thermal and Total mechanisms. The latter one is the sum of the Thermal, Prompt and N_2O mechanisms. (c) Time evolution of the Thermal's contribution degree to the Total NO prediction and temperature evolution. (d) Relationship between the Thermal NO and Thermal NO / Total NO for the three cases.

can be extracted. The first one is the time factor, which is very relevant in this process due to the different trends observed between cases. The second one is the T_{end} variable, which seems to be the main parameter affecting the NO formation, even though these conditions are located inside the LTC region.

In order to more representatively compare the different trends observed in the previous figures, two new plots, Figure 6(c) and 6(d), were designed and a new variable was defined, Thermal NO/Total NO. This variable quantifies the Thermal mechanism's predictive capability with respect to the Total NO prediction, obtained from simulating the All version of the San Diego model.

On one hand, Figure 6(c) illustrates the evolution of the Thermal's NO mechanism contribution degree to the Total NO prediction, as well as the temperature evolution of the three cases. As can be observed, the different trends seen in the previous figure turn into similar behaviour, despite the differences in temperature evolution between them. Generally speaking, all three cases start with a low initial Thermal contribution degree and temperature. As the combustion process evolves, both variables increase rapidly, especially temperature, converging to a constant value. Case B and Case C both have very similar Thermal contribution degree evolutions, but different temperature trends.

On the other hand, if the whole transient process (0–1 ms) is characterized as a function of Thermal NO, see Figure 6(d), all cases show identical behaviour, despite the differences between the temperature evolution of the three cases, as seen previously. Such a common trend reflects the existence of a relationship between both variables (Thermal NO/Total NO versus Thermal NO), which is independent of the considered working conditions, time variable and temperature evolution. If this relationship is confirmed for the rest of the cases, it can be very useful for modelling purposes. Finally, it is worth highlighting that Case A finishes much earlier than the others. The reason is due to the working conditions, represented in this case, which are not convenient for NO formation throughout the Thermal mechanism, and consequently, less than 60 ppm of NO is predicted in the whole calculation time (1 ms).

Global results

To confirm the relationship between Thermal NO prediction and its contribution degree to the Total NO prediction, previously observed, the rest of the cases were plotted under the same axis, Figure 7. As expected, when the time variable is discarded, identical behaviour was observed independently of the Z_r and T_{end} variables. The parametric study was enlarged by varying T_{ini} from 1400 K to 1300 K, and then to 1200 K. In all cases, identical trends were observed.

This fact corroborates the existence of such a relationship, independently of the combustion stage, over a wide range of working conditions. To relate both variables, a polynomial fit was calculated and drawn, see Figure 7(b). The fit obtained corresponds to a fourth-degree polynomial equation with an R^2 of 0.967 and was denoted as the corrective correlation

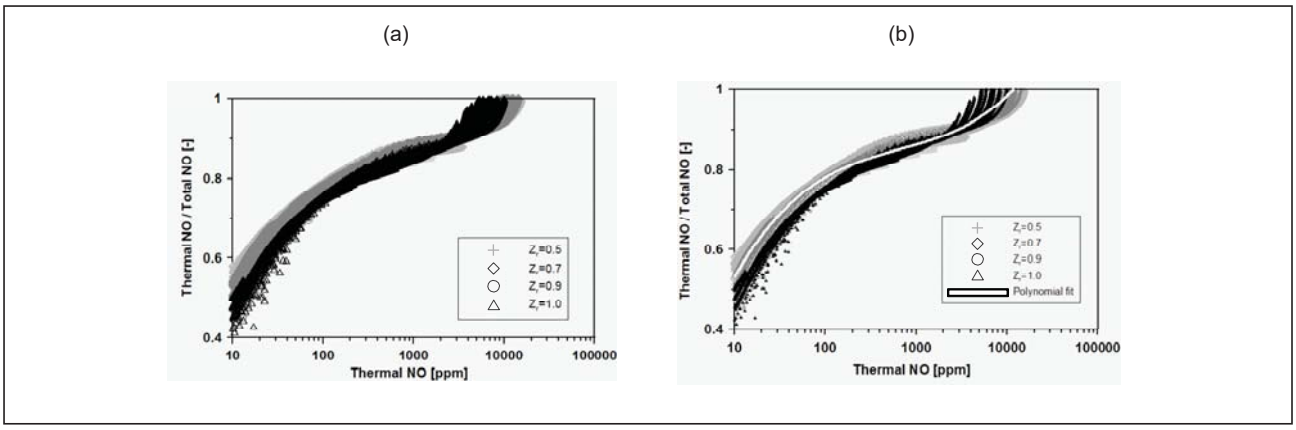

Figure 7. (a) Plot of all the cases analysed in this parametric study independently of their initial reaction temperature and relative mixture fraction. (b) Calculated polynomial fit for the results obtained for this parametric study.

$$\mathrm{Calc}\left(\frac{\text{Thermal NO}}{\text{Total NO}}\right) = -0.27 + 1.25\log(x) - 0.57\log(x)^2 + 0.12\cdot\log(x)^3 - 0.009\log(x)^4 \quad (1)$$

where x is the Thermal mechanism prediction in ppm units.

The corrective correlation (equation (1)) can be used to improve the NO predictions, by just using the Thermal NO formation mechanism, which has a low computational cost and is highly implemented in CFD software.

To check the effectiveness of this equation, the corrective correlation was applied throughout the whole evolution of the NO formation process for all the analysed local conditions, or in other words, at each instant of the NO evolution for every studied condition. Additionally, a new variable ((Total NO)$_{COR}$/ Total NO) was defined in order to quantify this effectiveness and was plotted versus the Thermal mechanism's prediction in Figure 8.

Generally speaking, it can be seen from Figure 8 that a substantial improvement of the predictive capability is obtained after applying equation (1), as the ((Total NO)$_{COR}$ /Total NO) coefficient is close to 1 throughout the whole NO range. This means that applying the corrective correlation to the Thermal mechanism's prediction yields similar values as if all three mechanisms were used to predict the NO formation.

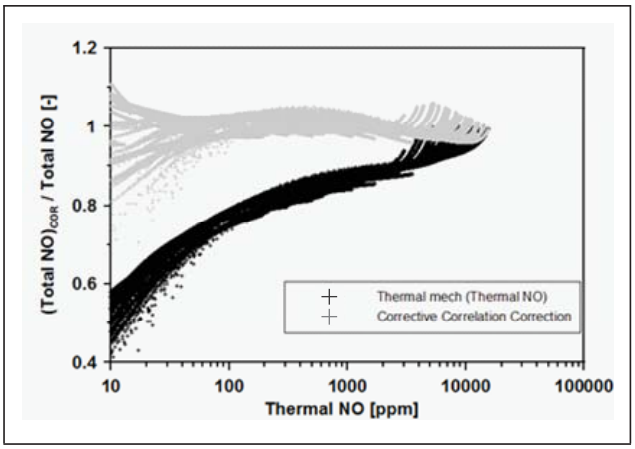

Figure 8. Comparison between the Thermal mechanism's predictive capability, before (black) and after (gray) applying the corrective correlation to every instant of the NO evolution process for every analysed local condition. The fuel employed was n-heptane.

Detailed analysis of this plot reveals that for LTC conditions (<40 ppm), the predictive capability has been substantially improved, even though high dispersion is observed, especially at very low NO formation conditions. However, for intermediate and high NO formation conditions (>40 ppm), the predictive capability of this methodology is extremely good and presents very low dispersion.

The profound analysis of the results obtained seems to yield one main factor: the creation of a law that is applicable to any local condition, described by T_{end}, Z_r, Y_{O2}, and for any instant in the NO formation process independently of the combustion stage. Consequently, this generality can be extrapolated to real NO formation processes in diesel sprays where continuously variable conditions are involved. However, this assumption will be explored in great detail in future work. Additionally, this law substantially improves the predictive capability of the Thermal mechanism, and can be easily implemented in current CFD and chemical-kinetic software to closely predict NO formation with no additional computational cost.

In order to validate this promising finding, a second single-component surrogate fuel was used, methane. The employment of methane also allows the study of the effects of a different fuel on the NO formation process.

The same methodology was used for this second fuel, and, as it can be seen in Figure 9, very small differences appear when comparing the Thermal mechanism's prediction for both fuels. The slightly lower predictive capability for methane can be explained due to a slight increase in the influence of the Prompt mechanism, which consequently leads to less NO formation due to the Thermal mechanism.

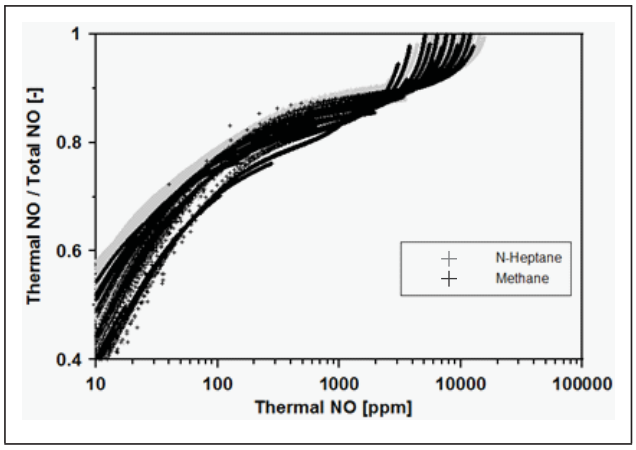

Figure 9. Comparison between the Thermal mechanism's predictive capability for n-heptane and methane over a wide range of working conditions.

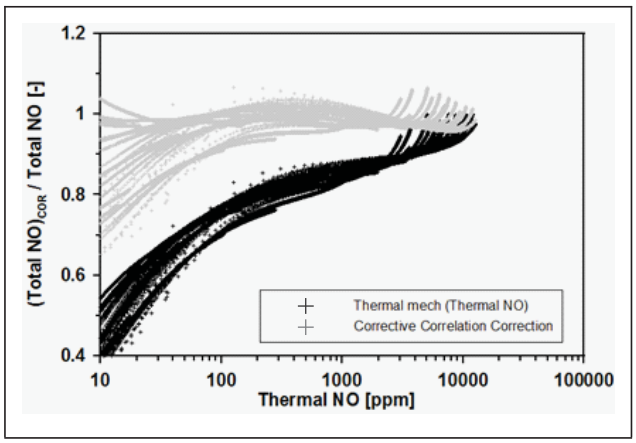

Figure 10. Comparison between the Thermal mechanism's predictive capability, with (gray) and without (black) applying the corrective correlation equation, considering all the studied cases of this parametric study employing methane as fuel.

As expected, applying the corrective correlation, unmodified, to the Thermal's prediction for methane reflects similar trends to those found for n-heptane, see Figure 10. Generally speaking, an increase in the predictive capability is observed throughout the whole NO range, even though it is for the medium and high range where the accuracy is greatest and the dispersion is lowest. For LTC conditions, a substantial increase in predictive capability is also achieved, but a higher dispersion degree is observed with respect to the n-heptane case.

Conclusions

After analysing the results obtained, the conclusions that can be extracted from the present study are the following.

1. The results obtained in the present study are in good agreement with the well-documented results in the scientific community for STD combustion scenarios. Under these conditions, the predicted NO emissions are traditionally related to the NO predicted by the extended Zeldovich mechanism (Thermal mechanism). As can be observed from Figure 8, the contribution degree of the Thermal NO formation mechanism is above 90% for Y_{O2} - 12.7% (Thermal NO >4000 ppm), making this mechanism ideal for closely predicting NO formation under STD combustions. However, when dealing with LTC combustion scenarios (Y_{O2} 4 12.7%), this mechanism reduces its contribution due to a reduction in combustion temperature, just as expected, and therefore reduces its capability of predicting NO formation. However, no relevant studies have been performed in order to compare the results obtained in the present study. This is the reason for the present study, especially when new combustion modes, characterized by LTC conditions, are being developed as a consequence of the stringent emission standards worldwide.
2. Due to new combustion technologies, such as LTC and HCCI, the use of the Thermal mechanism is inadmissible as the only predictive mechanism, especially if accurate simulations are required. The coupling of this mechanism with others, such as Prompt and N_2O intermediate, increases not only the accuracy of the NO prediction, but also the computational cost.
3. The relationship obtained between Thermal NO prediction and Thermal NO/Total NO coefficient, under very simplified conditions, yields a law that is applicable to any local condition, described by T_{end}, Z_r, Y_{O2}, and for any instant in the NO formation process independently of the combustion stage. Consequently, this generality can be extrapolated to real NO formation processes in diesel sprays where continuously variable conditions are involved. However, this assumption will be explored in future work. Additionally, this methodology substantially improves the predictive capability of the Thermal mechanism and can be easily implemented in current CFD and chemical-kinetic software to closely predict NO formation with no additional computational cost.
4. The previous findings were corroborated by also using methane as a fuel. This fact reflects the low influence of a different fuel. Nevertheless, the slight differences observed can be explained due to an increase in the influence of the Prompt mechanism. Finally, if the corrective correlation is applied to the Thermal mechanism's prediction, an increase in predictive capability is appreciated across the whole NO range.

Funding

The authors thank the Ministerio de Ciencia e Innovació n of the Spanish government for contributing to this work with the grant BES-2009-021897.

References

1. Dronniou N, Lombard B, Colliou T, et al. Dual-mode engine for Euro VI heavy-duty applications: presentation

of the concept. In: *Thiesel 2008 conference on thermo- and fluid dynamic processes in diesel engines*, 2008.
2. Dec JE. A conceptual model of DI diesel combustion based on laser-sheet imaging. *SAE Trans* 1997; 106: 1310–1348. SAE paper 970873.
3. Musculus M. Multiple simultaneous optical diagnostic imaging of early-injection low-temperature combustion in a heavy-duty diesel engine. SAE paper 2006-01-0079.
4. Zeldovich YB. The oxidation of nitrogen in combustion and explosion. *Acta Physicochim* 1946; 21: 577–628.
5. Merker GP, Hohlbaum B and Rauscher M. Two-zone model for calculation of nitrogen-oxide formation in direct-injection diesel engines. SAE paper 932454, 1993.
6. Fenimore CP (ed). Formation of nitric oxide in premixed hydrocarbon flames. In: *Proceedings of the 13th international symposium on combustion*, Pittsburgh, PA, 1971.
7. Turns SR. *An introduction to combustion: concepts and applications*. 2nd ed. Boston: McGraw-Hill, 1996.
8. Heywood JB. *Internal combustion engines fundamentals*. New York: McGraw-Hill, 1988.
9. Hernán dez JJ, Pé rez-Collado J and Sanz-Argent J. Role of the chemical kinetics on modeling NO emissions in diesel engines. *Energy Fuels* 2008; 22(1): 262–272.
10. Easley WL, Mellor AM and Plee SL. NO formation and decomposition models for DI diesel engines. SAE paper 2000-01-0582, 2000.
11. Yoshikawa T and Reitz RD. Development of an improved NOx reaction mechanism for low temperature diesel combustion modeling. SAE paper 2008-01-2413, 2008.
12. Amné us P, Mauss F, Kraft M, et al. NOx and N2O for- mation in HCCI engines. SAE paper 2005-01-0126, 2005.
13. Andersson M, Johansson B, Hultqvist A, et al. A real time NOx model for conventional and partially premixed diesel combustion. SAE paper 2006-01-0195, 2006.
14. Kohashi K, Fujii Y, Kusaka J, et al. A numerical study on ignition and combustion of a DI diesel engine by using CFD code combined with detailed chemical kinetics. SAE paper 2003-01-1847, 2003.
15. Lö ffler G, Sieber R, Harasek M, et al. NOx formation in natural gas combustion – a new simplified reaction scheme for CFD calculations. *Fuel* 2006; 85(4): 513–23.
16. Kee RJ, Rupley FM, Miller JA, et al. *Chemkin release 4.0*. Reaction Design Inc, San Diego, CA, 2004.
17. Peters N. *Turbulent combustion*. Cambridge: Cambridge University Press, 2000.
18. Akihama K, Takatori Y, Inagaki K, et al. Mechanism of the smokeless rich diesel combustion by reducing temperature. SAE paper 2001-01-0655.
19. Kook S, Bae C, Miles PC, et al. The effect of swirl ratio and fuel injection on CO emissions and fuel conversion efficiency for high-dilution, low temperature combustion in automotive diesel engines. SAE paper 2006-01-0197.
20. Opat R, Ra Y, Gonzalez MA, et al. Investigation of mixing and temperature effects on HC/CO emissions for highly diluted low temperature combustion in a light duty diesel engine. SAE paper 2007-01-0193.
21. Farrell JT, Cernansky NP, Dryer FL, et al. Development of an experimental database and kinetic models for surrogate diesel fuels. SAE paper 2007-01-0201, 2007.
22. Combustion Research Group at UC San Diego. *Chemical-kinetic mechanisms for combustion applications*. Department of Mechanical & Aerospace Engineering (Combustion Research), University of California at San Diego, http://maeweb.ucsd.edu/~combustion/cermech.

Appendix

Notation

$\mathrm{Calc}(\frac{\text{Thermal NO}}{\text{Total NO}})$	result of applying the LTC correction equation to the Thermal mechanism prediction
C_{fuel}	carbon mass in the fuel
C_{loca}	carbon mass at the specific location/ condition
C_{oxid}	carbon mass in the oxidizer agent
m_f	fuel mass
L_{liq}	evaporative liquid length
m_{oxid}	oxidizer mass (oxygen + EGR mass)
m_{O2}	oxygen mass
NO_x	nitrogen oxides
R^2	correlation coefficient
T_{end}	temperature reached at the end of the reaction
T_{ini}	initial temperature
Thermal NO	NO predicted by extended Thermal mechanism
$\frac{\text{Thermal NO}}{\text{Total NO}}$	Thermal contribution degree to the total NO formation
$\frac{(\text{Total NO})_{COR}}{\text{Total NO}}$	quantifies the effectiveness of the LTC correction equation by comparing the Thermal mechanism's prediction capability after applying the LTC correction equation
Total NO	NO prediction obtained from the San Diego model version taking into account the extended Thermal, Prompt and N_2O pathway mechanisms
Y_f	fuel mass fraction
Y_{O2}	oxygen mass fraction
$Y_{O2\ atm}$	atmospheric oxygen mass fraction
Z	mixture fraction
Z_r	relative mixture fraction
Z_{st}	stoichiometric mixture fraction

Abbreviations

CFD	computational fluid dynamics
EGR	exhaust gas recirculation
HCCI	homogeneous charge compression ignition
LOL	lift-off length
LTC	low-temperature combustion
PCCI	premixed charge compression ignition
PM	particulate matter
PSR	perfectly stirred reactor
STD	standard diesel combustion
USHC	unburned hydrocarbons